Trivent Publishing

Available online at http://trivent-publishing.eu/

Engineering and Industry Series
Volume *Power Systems, Energy Markets and Renewable Energy Sources in South-Eastern Europe*

CCT Estimation Based on Principal Components Analysis

Teodora Dimitrovska,[1] Urban Rudez,[2] Rafael Mihalic[3]

[1, 2, 3] Faculty of Electrical Engineering, University of Ljubljana, Slovenia,
teodora.dimitrovska@fe.uni-lj.si

Abstract

In recent years, a number of factors such as transitioning energy policies and slow transmission expansion have caused more frequent closing of operation of power systems due to their technical limits. Thus, the awareness of critical clearing time of contingencies, which is concerned with the ability of a power system to maintain synchronism after being subjected to a large disturbance, is gaining importance. On-line critical clearing time (CCT) estimation belongs to these types of applications, which give an extensive insight into system vulnerability, thus enabling early decisions and coordination of corrective control actions. This study presents a novel approach for estimating CCT applying data mining techniques. The proposal is tested on the IEEE New England 39-bus system. Results demonstrate the feasibility of the methodology in fast CCT estimation, suitable for on-line applications.

Keywords

CCT; data mining; estimation; transient; stability

I. Introduction

Historically, the problem of power-system stability first became pronounced in the case of long distance transmission where generating stations located remotely were feeding power to metropolitan load centers over long distances. High investments in automatic voltage regulators and high reactance transmission lines caused frequent operation near stability limits resulting in cases where loss of stability was a regular feature for any disturbance. Power transmission via weak tie-lines connecting large power systems was another occurrence where stability was of great concern [1]. In recent years, due to transitioning energy policies [2] and slow transmission expansion, power systems are frequently operated close to their technical limits. Additionally, large- scale deployment of renewable energy source generation, ranging from small to large highly-distributed units, has led to significant shares of variable power feed-in in power systems worldwide. Under these conditions, the vulnerability of the power system is significantly increased in selected pre-fault states as a result of reduced and heterogeneous inertia. Some contingencies traditionally considered negligible may now lead to major consequences, including widespread disruptions. These considerations call for a systematic a wide- area scale inquiry into the stability problem. Therefore, the approach to CCT estimation has shifted to fast, real-time applications in order to accommodate to the changing nature of electrical power systems operation. Several research works have been carried out with regards to CCT estimation in connection to transient stability assessment. Sources [3]-[8] include proposals whose aim is to perform fast transient stability assessment through novel, comprehensive approaches. In [3] the authors propose the use of transient energy functions in order to establish a relation between a reduced model, obtained from synchrophasor data, and a detailed model. CCT of contingencies of the reduced model provide an indication of the original system's stability margin. The technique is specifically developed regarding tie lines, therefore conclusions are presented on the basis of a two- machine equivalent system. An integrated approach to CCT calculation is presented in [4]. Energy function based analysis provides an approximation as input to a detailed time-domain simulation. Despite its accuracy, the method is not suitable for on-line applications, since average execution time exceeds the sub-second range, as presented in a case study. In [5], CCT estimation is carried out through direct methods. An analytically developed metric approximates the CCT metric. The key advantage

offered by this approach is the possibility for parametric variation (i.e. load variation). However, due to limitations of direct methods, connected to calculation of unstable equilibrium points (UEP), application is limited to the two-machine infinite bus (TMIB) system. In source [6] authors introduce the notation of projection energy function (PEF) in order to overcome the drawbacks of [7], [8] regarding identification of critical generator group and assessment of controlling unstable equilibrium point. A kinematic approach is applied to system trajectory, thus constructing a novel stability index. In this paper, a data-mining method is applied to fault-on rotor angles trajectories, with the scope of dimensionality reduction that facilitates a simple method for CCT estimation. The paper is organized as follows: Section 2 reviews the theoretical background on Center of inertia (COI)-referred machine angles as well as data mining method PCA. In Section 3, CCT estimation procedure is described, followed by a case study, presented in Section 4. Finally, Section 5 summarizes the concluding remarks.

II. Theoretical background

A. COI-referred rotor angles

The behavior of rotor-angle δi, regarding a synchronous machine in the power system is determined by the swing equation (1).

$$\frac{d\omega_i(t)}{dt} = \frac{1}{M_i}(P_{mi}(t) - P_{ei}(t)) \tag{1}$$

$$\frac{d\delta_i(t)}{dt} = \omega_i(t) - \omega_0 \tag{2}$$

Variables Mi, Pmi, Pei and ω_i stand for inertia moment, mechanical power input, electrical power output and rotor speed of the *i*th machine, respectively. Simulated time- domain trajectory of each machine angle is obtained as a solution of this differential equation. Equations (3) and (4) introduce the COI notation, where variable *M* is the total inertia moment, consisted of *n* machines, while δCOIi is the COI-referred rotor angle of *i*th machine. Since power systems can include machines of different sizes, the inertial influence of the system as a whole is best represented by the COI notion [1].

$$\delta_{COI} = \frac{1}{M}\sum_{i=1}^{n} M_i\delta_i \tag{3}$$

$$\delta_{COIi} = \delta_i - \delta_{COI} \quad (4)$$

The TSA criterion, regarding COI-referred rotor angles, establishes that, if rotor-angle of any machine or coherent area goes out of step after a fault is cleared (i.e. surpasses 180°), then the system is said to be first-swing unstable [1].

B. Principal Components Analysis

A pattern recognition technique, vastly used in facial recognition, was applied to fault-on trajectories of COI- referred rotor angles with the scope of dimensionality reduction. Principal component analysis is a data mining procedure that transforms a matrix of input variables (measurements) to a new, reduced set of variables called principal components. Newly obtained variables represent a linear combination of the original variables and are derived in decreasing order of importance given that the first principal component explains as much of the variation in the original data as possible. This transformation is in fact an orthogonal rotation in *m*-space, where *m* is the number of input parameters. Detailed description of PCA and possible applications can be found in [9], [10] and [11]. This mathematical approach is used in order to reduce dimensionality of data and enable visualization of covariance between input variables. A plot of the few output variables facilitates a visual understanding of the driving forces that generated the original data. Typically, an extensive amount of samples *n* contained in the database is described by a large number of variables *m*. Before PCA is applied all variables contained in the raw data matrix $\boldsymbol{Y}_{\mathrm{m\ x\ n}}$ are pre-processed by subtracting their respective mean and scaling them to unit standard deviation σ_{m}. This is the only pre-processing required so that data matrix $\boldsymbol{X}_{\mathrm{mxn}}$ consisting of *m* variables for *n* samples is obtained (where $m < n$):

$$x_{mj} = \frac{(y_{mj} - \overline{y_m})}{\sigma_m} \quad j = 1, \dots n \quad (5)$$

A full PCA decomposition reconstructs the measurement matrix as a sum over *m* orthonormal basis functions $\boldsymbol{w_1}'$ to $\boldsymbol{w}'_{\boldsymbol{m}}$ which are arranged as row vectors.

$$\boldsymbol{X} = \begin{pmatrix} t_{1,1} \\ \vdots \\ t_{m,1} \end{pmatrix} \boldsymbol{w}'_1 + \begin{pmatrix} t_{1,2} \\ \vdots \\ t_{m,2} \end{pmatrix} \boldsymbol{w}'_2 + \cdots + \begin{pmatrix} t_{1,m} \\ \vdots \\ t_{m,m} \end{pmatrix} \boldsymbol{w}'_m \quad (6)$$

Mathematically, $\boldsymbol{w}'$i vectors represent the normalized right eigenvectors of the *n* x *n* matrix $\boldsymbol{X}^{\mathrm{T}}\boldsymbol{X}$. The ratio between their respective eigenvalue and the sum of all the eigenvalues corresponding to their respective eigenvectors gives a measure

of the total variation captured by that eigenvector. Equation may be compactly written in matrix form:

$$\boldsymbol{X} = \boldsymbol{T}\boldsymbol{W}' \tag{7}$$

On the other hand, a description of the majority of the variations in $\boldsymbol{X}$ can be achieved by abbreviating the PCA description. The following equation is a two-dimensional PC model, where the variation of $\boldsymbol{X}$ that is not captured by the first two principal components appears in an error matrix $\boldsymbol{E}$.

$$\boldsymbol{X} = \begin{pmatrix} t_{1,1} \\ \vdots \\ t_{m,1} \end{pmatrix} \boldsymbol{w}_1' + \begin{pmatrix} t_{1,2} \\ \vdots \\ t_{m,2} \end{pmatrix} \boldsymbol{w}_2' + \boldsymbol{E} \tag{8}$$

The weighing of each principal component in each data variable of $\boldsymbol{X}$ may be represented graphically. When two components are used, *i*th observation corresponds to a point in a two-dimensional space called a scores plot. In this manner, trajectories of COI-referred machine angles are simultaneously presented in a two-dimensional scores plot. Despite the lack of obvious intuitive meaning, this decomposition offers simultaneous representation of *m* different input variables as one trajectory, which is constructed on the basis of covariance of input variables. In return, traits that are difficult to obtain in time-domain, due to high data dimensionality are now clearly underlined. In this section, an exemplary two-dimensional decomposition is depicted in Fig. 1. However, in sections 3 and 4, dimensionality is augmented to three dimensions, without loss of generality. Fig. 1 best illustrates the notations introduced in this section. Input variables are fault-on trajectories of machine angles of IEEE 39 bus system in a COI-reference frame, contained in raw input matrix $\boldsymbol{Y}_{\text{mxn}}$. After matrix $\boldsymbol{Y}$ is normalized, PC decomposition is executed. There are ten machines (m = 10) and six cases, in which fault clearing time varies from T_{clear} < CCT to T_{clear} > CCT. In order to improve time efficiency, fault simulations conducted in PSS® NETOMAC are aborted through batch processing, when either loss of stability is established (cases 5 and 6) or when a case is deemed first swing-stable (cases 1-4). Since only a single fault location scenario is considered in this section, system trajectory is represented in a two dimensional principle component-domain. The orthogonal axes, denoted in Fig. 1 as Component 1 and Component 2 correspond to the first two eigenvectors of covariance matrix $\boldsymbol{X}^{\mathrm{T}}\boldsymbol{X}$. Point-vectors D1 to D10 represent the first two rows of matrix Tmxm, while trajectories, illustrated as dotted lines are elements of matrix $\boldsymbol{W}$. In this manner, a novel approach to system variables observation is adopted. Some of the advantages offered by this proposal are discussed in this paper. In order to better understand the connection to the traditional time-domain representation,

trajectories of machine angles in case 6 ($T_{clear} \gg$ CCT) are also illustrated in Fig. 1 (top left corner). This framework allows considering several possible operating cases, observed through COI- referred machine angles. All of the cases follow the same trajectory, until fault is cleared. Each scenario starts from the fourth quadrant. However, cases where clearing time is less or equal to the CCT follow trajectories that also end in the fourth quadrant, as first swing is completed in time domain.

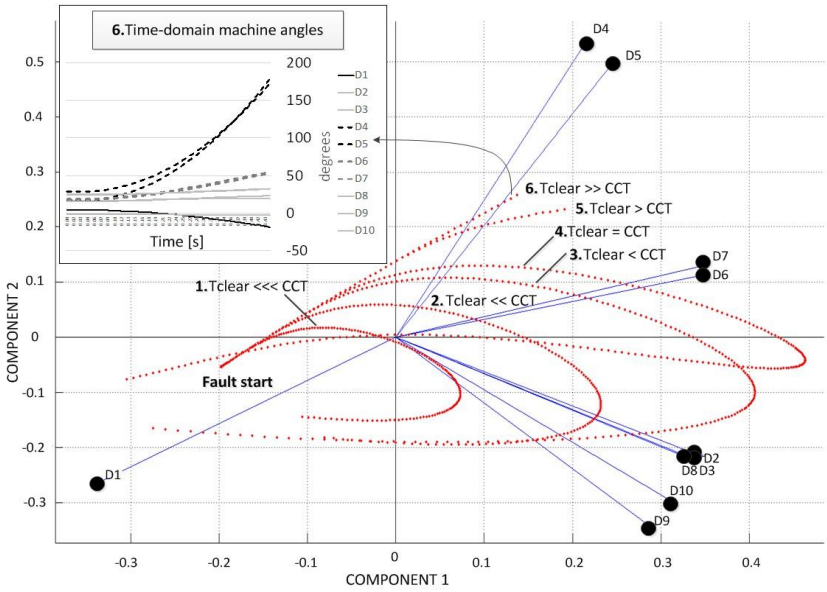

Fig. 1. Example of scores plot in two dimensions

III. CCT Estimation Proposal

The problem of first-swing stability is closely linked to angular separation between COI-referred rotor angles. Faults result in angular separation between groups of coherent machines. It is therefore of interest to research the possibility of providing a CCT estimation algorithm, based on PC decomposition of rotor angles and their relative positions in a novel components space. For that purpose, a database was created, consisting of fault-on rotor angles during several faults located at different buses. Once input data is decomposed to principle components, faults are differentiated into trajectory groups that fall into the same octant of components space. In order to obtain a detailed coherency understanding, trajectories in each octant are decomposed into principle components as well. Distance metric d^2 between each observation point $w(k)$ and machine angle coefficient t_i is defined as follows:

$$d_{ik}^2 = (w(k) - t_i)^T (w(k) - t_i)$$
$$1 \leq i \leq c,\ 1 \leq k \leq n \quad (9)$$

Subsequentially, Euclidean metric $d$ik is normalized according to (10) in order to gain a better understanding of the relative distance to machine coefficients, which in this context replace the notation of centroids, defined in fuzzy clustering problems.

$$\mu_i(k) = d_{ik}^2 \sum_{j=1}^{c} \frac{1}{d_{jk}^2}$$
$$\sum_{i=1}^{c} \mu_i(k) = 1\ \forall k \quad (10)$$

In this framework, centroids are fixed, since they are represented by machine coefficients, marked in Fig. 1 with black dots. However, relative distance to each centroid varies from observation to observation. Fig. 2 and Fig. 3 introduce the μ metric in reference to time-domain machine angle trajectories. It is evident that coherent machine groups have similar distance metrics that form clusters. Case 1 (Fig. 2) corresponds to fault presented in Fig. 1, where coherent machines 4 and 5 (marked with black, dashed lines) go out of step. Machines 2, 3, 8, 9, and 10 form a cluster of μ metrics, which is intercepted by the μ metrics of machines 4 and 5 near the CCT. In a different case (denotated as case 2, Fig. 3) machines 4-7, marked with a full, darker grey line, form a cluster of μ metrics. In time domain, these machines are a coherent group. Their relative distance metrics are averaged and considered as a single variable, without loss of generality. A similar observation is valid for machine cluster 2, 3, 8, 9, 10 while machine 1 represents a rigid source. The interception point of averaged μ metrics corresponding to groups from disjoint octants coincides with the CCT of the fault in both cases. Since μ is a distance metric, we can interpret x (t = CCT) as an observation that is characterized with intercepting distances to machines belonging to disjoint machine clusters. Since in general, distances intercept in more than one point, the point nearest CCT is identified as the observation x (k) with intercepting relative distance metrics between machine clusters with the largest coefficients (ti), as contained in matrix $\boldsymbol{T}$. For example, in case 1, Euclidean distance to cluster with the largest coefficient formed by machines 4 and 5 intercepts the distance to the second largest cluster, containing machines 2, 3, 8, 9, 10. A similar reasoning is applied in case 2. In order to test the general validity of this observation, a case study is performed, as follows.

IV. Case Study

The proposal is tested on the IEEE New England 39-bus system using PSS®NETOMAC for dynamic simulations and MATLAB for data mining. Three-phase short- circuit fault is applied to a random bus and it is left uncleared. Simulation is aborted once loss of stability is established. The process is repeated for 20 different buses in order to obtain a database matrix ***Y***, consisting of fault-on rotor angles. PC decomposition is followed by partition of faults to octants, and distance metrics calculation. Estimated CCT are presented in Table I. Discrepancy between estimated values and true CCT values does not exceed 10 ms. Cumulative execution time is consisted of simulation time (around 5 s), which prevails, while time range needed for CCT estimation is (0.343) or 0.0171 s per fault. Accuracy and execution time efficiency are comparable to fast energy functions based estimation proposals presented in sources [3]-[8].

V. Conclusion

A CCT estimation proposal was developed, based on a data mining technique that offers simultaneous representation of several input variables as a single trajectory, constructed on the basis of covariance of input variables. Traits that are not obvious in time-domain, due to high data dimensionality, are now clearly underlined. Estimated CCT coincides with intercepting distance metrics to disjoint machine groups. Time efficiency is comparable to fast, energy functions based algorithms. Results presented in this paper suggest that estimated values provide a close indication of true CCT. However the method was heuristically derived, based on extensive observations and its general validity should be the topic of further research. Algorithms. Results presented in this paper suggest that estimated values provide a close indication of true CCT. However the method was heuristically derived, based on extensive observations and its general validity should be the topic of further research.

Fig. 2. Case 1

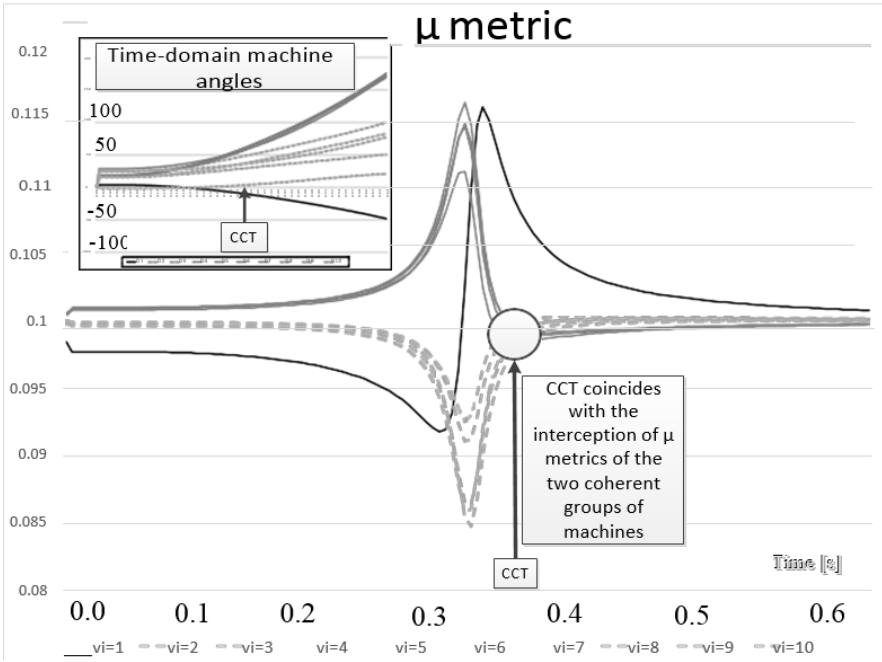

Fig. 3. Case 2

References

[1] M. Pavella, D. Ernst, and D. Ruiz-Vega. *Transient Stability of Power Systems: A Unified Approach to Assessment and Control*. Kluwer Academic Publishers, 2000.

[2] O. Feix, R. Obermann, M. Strecker, and A. Brötel. *German Grid Development Plan 2013*, (Netzentwicklungsplan Strom 2013). Berlin, 2013

[3] A. Paul and N. Senroy. "Critical clearing time estimation using synchrophasor data-based equivalent dynamic model." *Transmission Distribution IET Generation*, vol. 9, no. 7, pp. 609–614, 2015.

[4] B. K. Saharoy, A. K. Pradhan, and A. K. Sinha. "Computation of critical clearing time using an integrated approach," in *International Conference on Power Systems*, 2009. ICPS '09, 2009, pp. 1–5.

[5] L. G. W. Roberts, A. R. Champneys, K. R. W. Bell, and M. di Bernardo. "Analytical Approximations of Critical Clearing Time for Parametric Analysis of Power System Transient Stability." *IEEE Journal on Emerging and Selected Topics in Circuits and Systems*, vol. 5, no. 3, pp. 465–476, Sep. 2015.

[6] D. Z. Fang, J. G. Yang, W. Sun, Z. Y. Xue, and S. Q. Yuan. "Transient stability assessment using projection formulations." *Transmission Distribution IET Generation*, vol. 3, no. 6, pp. 596–603, Jun. 2009.

[7] Fang D.Z., David A.K. 'A normalized energy function for fast transient stability assessment', *Int. J. Electr. Power Syst. Res.*, 2004, 69, (2–3), pp. 287–293

[8] Fang D.Z., Song W.N., Zhang Y. 'A new transient energy function', *Sci. China Ser. E-Technol. Sci.*, 2002, 45, (4), pp. 426–432

[9] "A tutorial on Principal component Analysis" [Online]. Available: https://www.cs.princeton.edu/picasso/mats/PCA-Tutorial Intuition_jp.pdf [Accessed: March 14, 2016].

[10] N. F. Thornhill, S. L. Shah, B. Huang, and A. Vishnubhotla. "Spectral principal component analysis of dynamic process data." *Control Engineering Practice*, vol. 10, no. 8, pp. 833–846, Aug. 2002

[11] B. Moore. "Principal component analysis in linear systems: Controllability, observability, and model reduction." *IEEE Transactions on Automatic Control*, vol. 26, no. 1, pp. 17–32, Feb. 1981

Table 1

Bus	***Estimated CCT (s)***	***True CCT (s)***	***Absolute error (s)***	***Relative error (%)***
29	0.177	0.167	0.01	5.99
28	0.180	0.172	0.008	4.65
6	0.212	0.202	0.01	4.95
5	0.222	0.212	0.01	4.72
19	0.207	0.217	-0.01	-4.61
16	0.262	0.252	0.01	3.97
7	0.242	0.252	-0.01	-3.97
8	0.242	0.252	-0.01	-3.97
11	0.252	0.257	-0.005	-1.95
10	0.267	0.272	-0.005	-1.84
4	0.282	0.277	0.005	1.81
22	0.297	0.287	0.01	3.48
23	0.297	0.292	0.005	1.71
13	0.287	0.297	-0.01	-3.37
24	0.312	0.307	0.005	1.63
14	0.312	0.312	0	0.00
17	0.307	0.317	-0.01	-3.15
21	0.322	0.322	0	0.00
15	0.362	0.362	0	0.00
18	0.405	0.402	0.003	0.75
CPU(s)	5.343 (0.267 per fault)			